P H Y S I C A L   R E V I E W   L E T T E R S

Intermixing of Intrabasin and Interbasin Diffusion of a Single Ag Atom on Si(111)-(7 × 7)

Kedong Wang,[1,2,*] Gang Chen,[2] Chun Zhang,[2] M. M. T. Loy,[2] and Xudong Xiao[1,2,*]

[1]*Department of Physics, The Chinese University of Hong Kong, Shatin, New Territory, Hong Kong, China*
[2]*Department of Physics, Hong Kong University of Science & Technology, Hong Kong, China*

Using scanning tunneling microscopy, we studied the diffusion of single Ag atoms within the Si(111)-(7 × 7) unit cell. A striking difference was observed in the time-dependent tunneling current spectra for Ag atoms moving in the unfaulted and faulted half unit cells, with a dual-time characteristic in the former but a single time in the latter. Our observations demonstrate the importance of the stacking fault in affecting the interaction between Ag atoms and the Si(111)-(7 × 7) surface and can be understood in terms of an asymmetric interplay between intrabasin and interbasin diffusion.

Surface diffusion is an important subject in many physical processes including thin film growth and nanostructure formation at surfaces and has continually attracted great attention in recent research [1–4]. As a popular semiconductor substrate for metal thin films [5–7] and a unique template for self-assembly of nanostructures [8–10], Si(111)-(7 × 7) surface and its interaction with atoms and molecules have been intensively studied. Among various metallic elements, Ag on Si(111)-(7 × 7) forms a model system for the study of metal-semiconductor interface and Schottky barrier formation [5] because Ag does not react with Si and forms an abrupt interface [11]. While numerous studies have already been made in silver film growth on Si(111)-(7 × 7), the dynamics of Ag atoms, in particular, at the initial growth stage, remain poorly understood [12,13]. Understanding of diffusion behavior and the potential energy surface (PES) is critical for the control of growth of thin films and nanostructures.

According to the dimer-adatom-stacking fault (DAS) model [14], a unit cell of the Si(111)-(7 × 7) reconstruction consists of a faulted half unit cell (FHUC) and an unfaulted half unit cell (UHUC). The atomic structures of the top Si surface layers in the two halves are basically mirrored with respect to the line through the Si dimer rows. Because the stacking fault is between the third and forth Si layers from the surface, its effect on the adsorbates is usually negligible except an overall lowering of potential energy in FHUC [10,15–17]. For example, first principles calculations with a full Si(111)-(7 × 7) unit cell found no difference in adsorption sites and a small difference (<10%) in diffusion barriers for Pb [15], Na [16], and Si [17] in the two half unit cells. Experimental diffusion results of Pb [15], Na [16], H [18], and O₂ [19] in FHUC and UHUC also revealed only ~10% difference in the diffusion barriers, close to the experimental uncertainty. Our early calculations and experiments for Cu, Ag, and Au single atoms on Si(111)-(7 × 7) indicated some difference in the adsorption energy in the two half unit cells [20], but the implication on the surface dynamics from the adsorp-

tion energy landscape difference as well as the diffusion barriers remain unexplored.

In this Letter, we report an observation of strong asymmetric dynamic behavior of Ag atoms in FHUC and UHUC which has not been seen before for any other atoms: a dual-time scale for diffusion dynamics for Ag atoms in UHUC, but not in FHUC. From a PES calculated by first principles method, we can attribute the dual-time scale behavior in UHUC to be mixture of intrabasin and interbasin diffusion, while the single-time scale behavior in FHUC is due to interbasin diffusion alone, with the intrabasin diffusion highly suppressed. Here a basin is defined by a triangle with the rest Si atom at the center and three surrounding Si adatoms at the corners [21,22]. Our findings clearly demonstrate that the stacking fault can lead to an observable and significant consequence for the surface dynamics in addition to the PES corrugation.

Our experiment was carried out with an Omicron variable temperature scanning tunneling microscope (STM) operated in ultrahigh vacuum (base pressure ~7 × 10⁻¹¹ torr). The STM tips were chemically etched tungsten tips, which, prior to their first use, were sputtered with Ar⁺ to remove the oxidation layer. The Si(111) wafer was *p*-type with a room temperature resistivity of 7 Ω · cm. After a thorough degassing at ~900 K for several hours, the clean Si(111)-(7 × 7) surface was prepared by repetitively flashing to ~1500 K under a vacuum of <2 × 10⁻⁹ torr. A small amount of Ag, ~0.002 monolayer as evaluated directly from STM images, was then deposited to the clean Si(111)-(7 × 7) surface at room temperature. During the STM measurement, the sample temperature was controlled by a combination of cooling and heating. We used a time-dependent tunneling spectroscopy method [23] to detect the fast motion of Ag atom on Si(111)-(7 × 7). Briefly, we placed an STM tip at a fixed position (e.g., above a stable adsorption site) under which a diffusing atom may repeatedly pass through. By measuring the tunneling current as a function of time with the feedback loop disabled, the residence time and thus the hopping rate

of the atom at an adsorption site can be deduced. This method can detect diffusion motion at least about 2–3 orders of magnitude faster than video STM [23] and is capable of acquiring a large number of events (~200–500) within a reasonable time period for good statistics. To minimize the STM tip effect, we operated the STM at 50 pA with various bias voltages, ensuring a tip-surface distance ~1.0 nm as judged by the measured tunnel current versus tip-surface distance curves.

Figure 1(a) shows a room temperature STM image of Ag atoms on Si(111)-(7 × 7). Even when there is only one single Ag atom occupying FHUC or UHUC, the STM image shows six bright (brighter than Si adatoms) spots forming a triangle [6,13]. After cooling the sample to 77 K [Fig. 1(b)], the Ag atom in FHUC becomes immobile and shows only one bright spot at the corner Si-adatom position, while the Ag atom in UHUC remains hopping at a reduced rate. This change in STM images between room temperature and low temperature was found reversible, indicating that the six bright spots at room temperature is a result of frequent hopping of the Ag atom among different adsorption sites.

To quantify the dynamics of Ag atoms in the respective half unit cells, we measured the temperature dependent hopping rate. In Fig. 2(a), a typical two-state tunneling current signal in time is shown for the STM tip positioned stationary over a corner Si-adatom site in FHUC [position a in Fig. 2(e)] at 144 K. The high current (~250 pA) corresponds to an Ag atom residing at a site associated with the bright spot at the corner Si-adatom, while the low current (~50 pA) corresponds to the Ag atom away from this site. From many such two-state current signals, we obtained the ratio of the total residence time of one single Ag atom "under" the STM tip over the total measurement time. This ratio is ~33%, consistent with a picture that the Ag atom diffuses with equal probability to three stable adsorption sites. The average residence time τ and the hopping rate $\Gamma = 1/\tau$ can then be obtained from the statistics of the distribution of residence time at a given site [23].

In UHUC, however, the dynamic behavior is completely different, as can be seen in Fig. 2(b) with the tip positioned
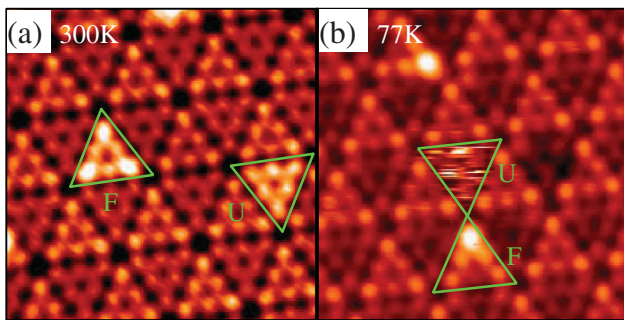
over a corner Si-adatom site as above but now on the UHUC side. While the low current state is similar to that in (a), one now sees a very "noisy" high current state that oscillates between the current baseline and the current maximum. This dual-time scale behavior is also present in Fig. 2(d) where the tip is positioned over a center Si adatom in UHUC. Figures 2(f) and 2(g) show, respectively, portions of Fig. 2(b) and 2(d) at faster time scale exhibiting that the "noise" in fact consists of spectra similar to those of Fig. 2(a) but at a much shorter time scale.

To understand what causes the different dynamic behavior for Ag atoms in UHUC and FHUC, we calculated the static potential energy surface for Ag on Si(111)-(7 × 7), as shown in Fig. 3(a), by first principles method based on the density functional theory (DFT) [24,25] with the Vienna *ab initio* simulation package [VASP] [26,27]. In the calculations, a repeated slab geometry is used, with six Si layers separated by a 12 Å vacuum to eliminate the interaction of adsorbed atoms with the periodic images of surface. The unit cell consists of 298 Si atoms in the DAS model and 49 H atoms that terminate the bottom Si layer. The wave functions are expanded in a plane wave basis with an energy cutoff of 250 eV. Only the Γ point is used in the summation of the Brillouin zone of simulation cell. The silicon atoms in the bottom layer of the unit cell are fixed to model the bulk lattice, while all the other atoms are fully
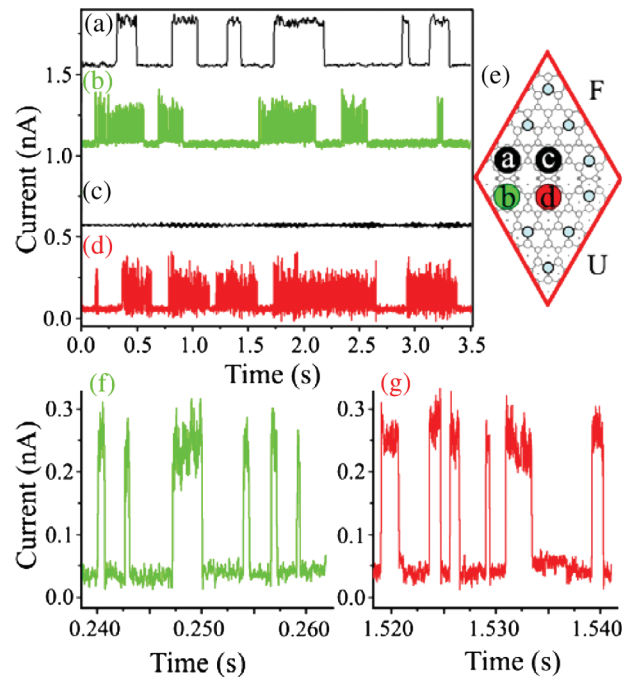
FIG. 2 (color).   (a) and (c) Typical time-dependent tunneling spectra taken at 144 K for an STM tip above the corner and center Si-adatom, respectively, in a FUHC containing a moving Ag atom. (b) and (d) Typical time-dependent tunneling spectra at 106 K for an STM tip above the corresponding sites in a UHUC with a moving Ag atom. (e) Schematics for the STM tip positions to acquire the spectra in (a) to (d). (f) and (g) Zoom-in of the dense noisy spectra in (b) and (d), respectively.

FIG. 1 (color).   STM images of single Ag atoms on Si(111)-(7 × 7) at (a) 300 K and (b) 77 K, taken at a tunneling current of 50 pA and a sample bias of −2.0 V. The FUHC and UHUC with Ag atoms are labeled.
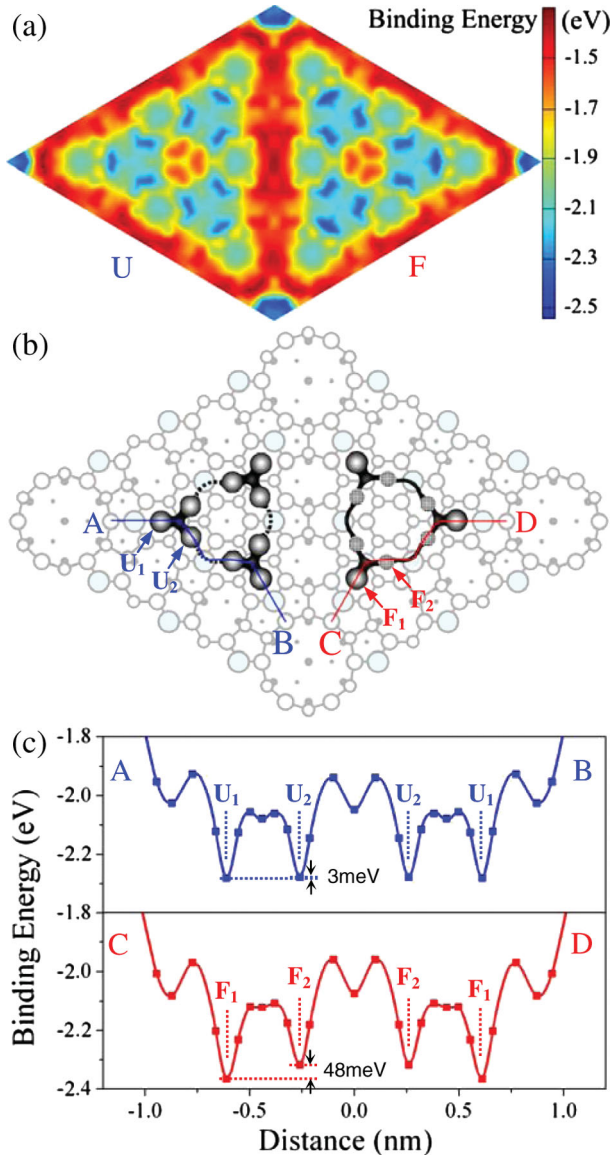
FIG. 3 (color). (a) A potential energy surface for a Ag atom on Si(111)-(7 × 7) constructed by first principles calculations. (b) The adsorption sites and the probable diffusion paths for Ag atom in the two half unit cells, with the DAS model of a clean Si(111)-(7 × 7) surface displayed in the background. (c) Potential energy along the paths outlined in (b) for both FUHC and UHUC.

relaxable. The optimization is stopped when the forces acting on each atom reach the tolerance of 0.02 eV/Å [28].

As seen in Fig. 3(a), the lowest energy sites are near the H_3 sites instead of the Si-adatom sites, in spite of at which the bright spot was observed in STM images at negative bias [20]. Inside a basin, there are three potential energy wells at which the Ag atom may reside. At elevated temperatures, the Ag atom may diffuse frequently among these three sites. Diffusion among different basins is also possible, but at a lower rate. This picture was originally proposed by Cho and Kaxiras [21,22] from their calculations using a (4 × 4) unit cell but has seldom been experi-

mentally verified [29]. In this picture, there are naturally two time scales for the Ag atom in each half unit cell and can explain well the observation in UHUC. When the tip is placed above a corner Si-adatom [position b in Fig. 2(e)], only one basin is detected. However, when the tip is placed above a center Si-adatom [position d in Fig. 2(e)], two neighboring basins are detected. Thus, the lower current level in Fig. 2(b) and 2(d) corresponds to Ag atoms diffusing away from the basin(s) being detected, while the high current level with filled "noise" corresponds to Ag diffusion within the basin(s) being detected. This explains why there were about 30% of time in Fig. 2(b) with noisy high current when effects from one out of three basins is detected, and about 70% of time in Fig. 2(d) with noisy high current when effects from two out of three basins are detected.

In principle, a similar dual-time scale behavior should also be observed for Ag diffusion in FHUC. The null observation is due to differences in adsorption energy landscape at the adsorption sites and the corresponding dynamics. The adsorption energies at $U1$ and $U2$ sites in UHUC (Fig. 3) differs by <5 meV as determined from both experiment and theory. On the FHUC side, the adsorption energies at the corresponding $F1$ and $F2$ sites have a much large difference, apparently caused by the stacking fault underneath. Experimentally, from a large number of sequential STM images at low temperature (122 K) and a large number of time-dependent tunneling current spectra at higher temperatures [e.g., Fig. 2(c)], no events for Ag at $F2$ was found, setting a limit of the ratio of residence time in $F1$ and $F2$ sites >1000, implying an adsorption energy difference to be >80 meV. The theoretical calculation confirms such a trend in adsorption energy and gives a difference of 48 meV [Fig. 3(c)]. This difference in adsorption energy could render the residence time of Ag atom at $F2$ sites too short to be detected. Effectively, the Ag atom appears to reside only at $F1$ before hopping out to another basin.

Thus, in analyzing the time-dependent tunneling spectra, for Ag in UHUC we have two hopping processes: one for intrabasin diffusion and the other for interbasin diffusion; but for Ag in FHUC, we need only to consider interbasin diffusion. The results are plotted in Arrhenius form in Fig. 4 for a wide range of temperatures. Using $1/\tau = \nu_0 \exp(-E_a/kT)$, the interbasin diffusion in FHUC and UHUC have comparable activation energy of $E_a = 0.27 \pm 0.02$ eV and 0.24 ± 0.03 eV respectively. While the prefactor in UHUC ($\nu_{0U} = 10^{12.3\pm0.5}$ s^{-1}) is normal, the prefactor in FHUC is 2 orders of magnitude lower ($\nu_{0F} = 10^{10\pm0.3}$ s^{-1}), possibly originated from complicated diffusion pathway. The measured interbasin hopping rates differ by $\geq 10^3$ times in the two half unit cells for the overlapping temperatures, an asymmetry that has never been observed before. The intrabasin fast diffusion in UHUC has an $E_a = 0.12 \pm 0.03$ eV, a value much smaller than that between two basins. The accompanied small prefactor $\nu_0 = 10^{8.7\pm0.5}$ s^{-1} is consistent with the com-
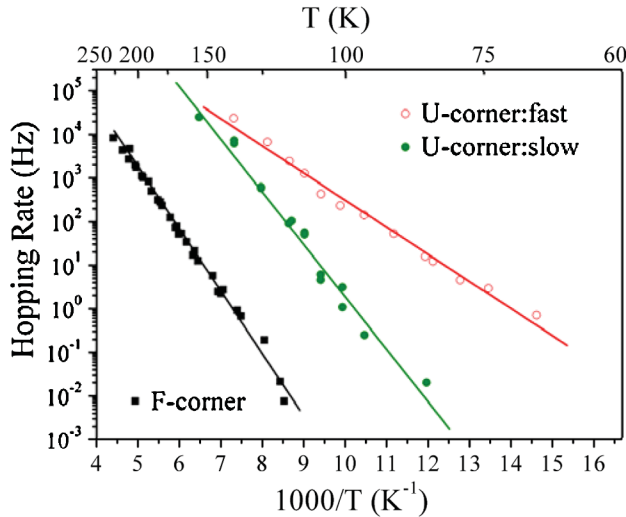
FIG. 4 (color).   Arrhenius plots of the hopping rate, $1/\tau$, for Ag atoms in FHUC and UHUC. The data obtained at different bias (-0.5 to -2.5 V) in FUHC show no bias dependence. The data shown for UHUC are obtained for STM positioned above a corner Si adatom at a bias of -0.5 V to minimize electric field effect.

pensation effect as generally found in thermal activation processes [30] and might reflect the complicated nature of the diffusion path. The first principles calculations are in good agreement in the overall trend, giving a barrier for interbasin diffusion 0.40 eV in FHUC and 0.34 eV in UHUC, and an intrabasin diffusion barrier of 0.23 eV in UHUC. However, all these values are somewhat higher than the measured ones. The accuracy of the DFT method, the noninclusion of finite temperature entropic and dynamic effects by the DFT calculation may contribute to the over-estimations of activation energies. Our experimental observations are in strong contrast to the existing experimental data of many other adsorbates on this surface, such as Pb [15], Na [16], H [18], O_2 [19] and Si [31] for which no strong asymmetry for diffusion rate or diffusion behavior in the two halves was reported.

In summary, we have observed a strong and interesting asymmetric dynamic behavior for Ag atoms moving in the two half unit cells of Si(111)-(7 × 7). With the help of PES constructed by first principles calculations, we can well explain the dual-time scales in UHUC as an intermixing of intrabasin and interbasin diffusion. The different adsorption energies and dynamics among adsorption sites in FHUC render the intrabasin diffusion unobservable and only exhibit the interbasin dynamics. This places Ag into a distinct class of adsorbates on Si(111)-(7 × 7) and provides a unique example that demonstrate a subtle asymmetry from the stacking fault in Si(111)-(7 × 7) unit cell can cause appreciable asymmetry in adsorption energy and dramatic difference in dynamic behavior.

*Corresponding authors.
kdwang@phy.cuhk.edu.hk
xdxiao@phy.cuhk.edu.hk

[1] K. R. Roos *et al.*, Phys. Rev. Lett. **100**, 016103 (2008).
[2] T. Tansel and O. M. Magnussen, Phys. Rev. Lett. **96**, 026101 (2006).
[3] I. Brihuega, M. M. Ugeda, and J. M. Gómez-Rodríguez, Phys. Rev. B **76**, 035422 (2007).
[4] E. Wahlstrom *et al.*, Science **303**, 511 (2004).
[5] W. Monch, *Semiconductor Surfaces and Interfaces* (Springer-Verlag, Berlin, 2001).
[6] St. Tosch and H. Neddermeyer, Phys. Rev. Lett. **61**, 349 (1988).
[7] H. M. Zhang, K. Sakamoto, and R. I. G. Uhrberg, Phys. Rev. B **64**, 245421 (2001).
[8] L. Vitali, M. G. Ramsey, and F. P. Netzer, Phys. Rev. Lett. **83**, 316 (1999).
[9] M. Y. Lai and Y. L. Wang, Phys. Rev. B **64**, 241404(R) (2001).
[10] J. L. Li *et al.*, Phys. Rev. Lett. **88**, 066101 (2002).
[11] E. J. Leonen *et al.*, Surf. Sci. **137**, 1 (1984).
[12] T. Jarolímek *et al.*, Surf. Sci. **482–485**, 386 (2001).
[13] P. Sobotík, P. Kocán, and I. Ošťádal, Surf. Sci. **537**, L442 (2003).
[14] K. Takayanagi *et al.*, Surf. Sci. **164**, 367 (1985).
[15] O. Custance *et al.*, Phys. Rev. B **67**, 235410 (2003).
[16] K. Wu *et al.*, Phys. Rev. Lett. **91**, 126101 (2003).
[17] C. M. Chang and C. M. Wei, Phys. Rev. B **67**, 033309 (2003).
[18] R.-L. Lo *et al.*, Phys. Rev. Lett. **80**, 5584 (1998).
[19] I.-S. Hwang, R.-L. Lo, and T. T. Tsong, Phys. Rev. Lett. **78**, 4797 (1997).
[20] C. Zhang *et al.*, Phys. Rev. Lett. **94**, 176104 (2005).
[21] K. Cho and E. Kaxiras, Europhys. Lett. **39**, 287 (1997).
[22] K. Cho and E. Kaxiras, Surf. Sci. **396**, L261 (1998).
[23] K. D. Wang *et al.*, Phys. Rev. Lett. **94**, 036103 (2005).
[24] P. Hohenberg and W. Kohn, Phys. Rev. **136**, B864 (1964).
[25] W. Kohn and L. J. Sham, Phys. Rev. **140**, A1133 (1965).
[26] G. Kresse and J. Hafner, Phys. Rev. B **47**, 558 (1993).
[27] G. Kresse and J. Furthmüller, Phys. Rev. B **54**, 11 169 (1996).
[28] With a subtle mistake in the real space projection scheme removed in the new VASP code, the accuracy of calculations is improved. See http://cms.mpi.univie.ac.at/vasp.
[29] H. F. Hsu *et al.*, Phys. Rev. B **68**, 165403 (2003).
[30] Y. L. Khait *et al.*, Phys. Rev. B **50**, 14 893 (1994) and references therein.
[31] T. Sato, S. Kitamura, and M. Iwatsuki, J. Vac. Sci. Technol. A **18**, 960 (2000).